Journal of Nano- and Electronic Physics
Vol. **10** No 5, 05038(5pp) (2018)

Журнал нано- та електронної фізики
Том **10** № 5, 05038(5cc) (2018)

Dip Coated ZnO Films for Transparent Window Applications

Meenakshi[1], Sanjay Kumar[1], Sudhir Saralch[1], Naresh Dhiman[1], Manish Kumar[2], Dinesh Pathak[1,*]

[1] *Department of Physics, Sri Sai University Palampur, India*
[2] *Department of Chemistry, Sri Sai University Palampur, India*

(Received 19 July 2018; revised manuscript received 22 October 2018; published online 29 October 2018)

ZnO is widely used as a functional material because it has a wide and direct band gap, large excitons binding energy, and excellent chemical and thermal stability. ZnO is a semiconductor material which is widely used as transparent electrodes in solar cells, chemical and gas sensors and light emitting diodes, due to its unique electrical and optical properties. Zinc oxide (ZnO) thin films were deposited on glass substrate by dip coating technique. The effects of sol aging time on the deposition of ZnO films were studied by using the field emission scanning electron microscopy (FE-SEM) and optical transmission techniques. Thin films of ZnO were prepared on glass substrate and annealed at 300 °C, 350 °C and 400 °C. The increase in sol aging time resulted in a gradual improvement in crystallinity. Effect of sol aging on optical transparency is quite obvious through increased transmission with prolonged sol aging time. Interestingly, 72-168 h sol aging time was found to be optimal to achieve smooth surface morphology, good crystallinity and high optical transmittance which were attributed to an ideal stability of solution. The UV-Vis transmittance spectrum of synthesized sample suggests the optical band gap value of 3.2 eV. Dip coating technique create ZnO films with potential for application as transparent electrodes in optoelectronic devices such as solar cell.

Keywords: TCO, Dip coating, Structural properties, Band gap.

DOI: 10.21272/jnep.10(5).05038 PACS numbers: 68.55. − a, 68.37.Hk

1. INTRODUCTION

Zinc oxide is one of the versatile and technologically interesting semiconducting material because of its typical properties such as resistivity control over the range 10^{-3}-10^{5} Ω cm [1], transparency in the visible range, high electrochemical stability, direct band gap (3.3 eV), absence of toxicity and abundance in nature. It crystallizes in a wurtzite structure and exhibits *n*-type conductivity due to residual donors [2]. Stoichiometric ZnO films are highly resistive, but less resistive films can be made either by introducing oxygen vacancies which act as donors or by doping with group III elements as Al, Ga or In [3].

ZnO is one of the semiconductors having good chemical stability against hydrogen plasma [4] and suitable for photovoltaic applications because of its high-electrical conductivity and optical transmittance in the visible region of the solar spectrum [5], which is primarily important in solar cell fabrications. Thin films of ZnO can be used as a window layer and also as one of the electrodes in solar cell [4]. Along with this application, ZnO thin films have been used in varistors [6], gas sensors [7] and solar cell transparent contact fabrication [8] etc.

ZnO thin films have been prepared by a variety of thin-film deposition techniques, such as pulsed laser deposition [9], RF magnetron sputtering [10], chemical vapour deposition [11], spray pyrolysis [12], electrodeposition [13] and sol-gel process [14, 15] etc.

Among them, the sol-gel technique offers the possibility of preparing a small as well as large-area coating of ZnO thin films at low cost for technological applications. In this work, thin films of ZnO were prepared by sol-gel associated with dip coating onto glass substrates. Structural and optical characterizations of ZnO thin films are reported.

2. EXPERIMENTAL DETAILS

Sol gel method was used to prepare zinc oxide thin film. Zinc acetate dihydrate ($Zn(CH_3COO)_2 \cdot 2H_2O$), absolute ethanol and distilled water (H_2O) were used as a starting material, dissolving 2.2 g of zinc acetate dehydrate in 40 ml of distilled water, after which the solution was stirred vigorously using a magnetic stirrer for 30 minutes on a hot plate at 60 °C to obtain homogeneous solution. After dissolving ethanol and potassium hydroxide, heated at 60 °C for 1 hr and finally zinc acetate solution added into homogeneous solution. Initially the solution was milky but after stirring for approximately 2 hr at 60 °C, the solution became homogeneous, transparent and stable. The sol was aged for 24 hours and then dip-coating was carried out.

In this experiment glass substrates were used. The substrates were washed with a detergent and ultrasonically cleaned in acetone and then in isopropanol. Thin film of ZnO were deposited on glass substrate obtained from blue star, India. Each layer of as prepared film was dried at 300 °C and 350 °C in oven for 20 minutes. The dipping process was conducted four times after each layer cooled down at room temperature.

For second recipe, 1.0 g polyvinyl alcohol was added to the homogeneous solution as a capping agent, stirring this solution for 1hr at 60 °C and aged at room temperature for 24 hr. Finally this solution was dip coated on the glass substrate with for drying and heating at same temperature as reported above.

3. RESULTS AND DISCUSSION

3.1 Scanning Electron Microscope

SEM micrographs were taken at different resolutions and resultant SEM images are shown in Figure 1, Figure 2 and Figure 3.

Figure 1 (a) shows the SEM images of the ZnO mul-

tilayer thin film prepared at different temperatures i.e. 300 °C, 350 °C and 400 °C. Sample has been synthesized at 300 °C for 60 min without any additional agent. The surface of the sample is smooth and uniform and a network structure is formed. Micro structural analysis of ZnO thin film sample prepared at temperature 300 °C was carried out using Scanning electron microscope (SEM). The layers do not overlap and there is a light trapping structure on the surface. This structure can enhance the reflection of the sunlight, lengthen the optical distance of the sunlight in the thin film and improve the photoelectric conversion efficiency as compared with the literature [16]. The grains of the thin films have been formed with uniform and loose surface.

During the coalescence stage of the dip coating process, fine particles do not have enough kinetic energy to grow into larger grains [17].

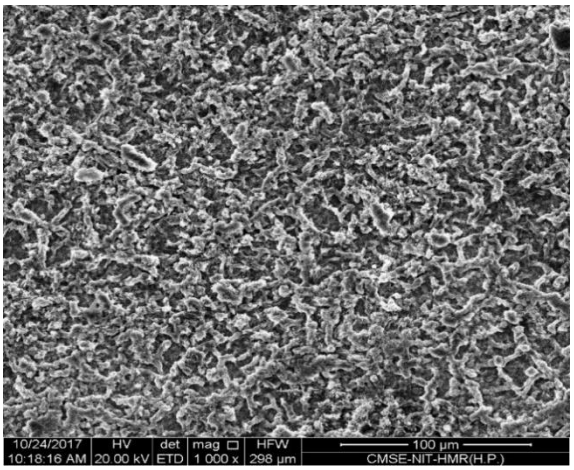

a

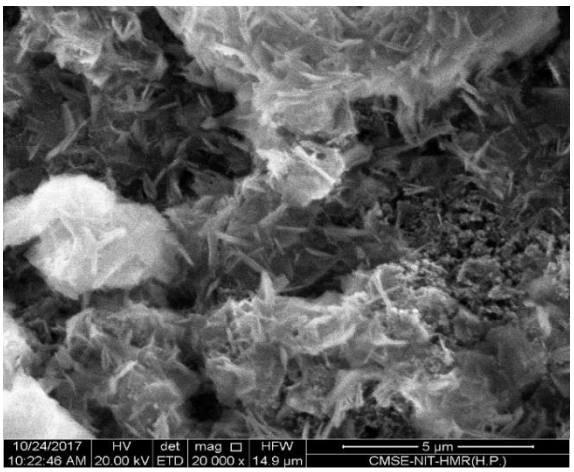

b

Fig. 1 – SEM images of ZnO thin film sample prepared at temperature 300 °C

From the Figure 1 (b) images shows that nanoplates of ZnO have been produced at 300 °C. This behavior may be attributed to the fact that the growth kinetic process of ZnO is slow at low temperatures, so the growth of nano species takes place at higher temperature to obtain different morphological structures. However, rise in reaction temperature results in increase in reaction rate, so ZnO grains rapidly grow, which leads to formation of nanorods with random orientations at 300 °C.

The morphology evolution of ZnO as influence of temperature is due to nanorods getting squeezed together to form nanoparticles [18]. At higher temperature, 300 °C, nanoplates have been obtained and size of these nanoplates is 1 µm. So, the most proper reaction temperature is that which produces uniform size distribution of ZnO nanorods with high aspect ratio of 300 °C as compared with the literature [19]. This creates great amount of ZnO nuclei and limits the crystal growth rate, and then large-scale hexagonal ZnO particles were produced. The grain size of the film vary between 1-6 µm. So, the most proper reaction temperature is that which produces uniform size distribution of ZnO nanorods with high temperature as compared with the literature [20].

Figure 2 (a) suggest SEM images of the ZnO thin films sample prepared at temperature 350 °C. Figure 2 (a) shows granular like shape of the grains. Effectively, the as-prepared film produces the appearance of a gra nular structures composed of small grains that appear somehow aggregated with porosity around. The growth of unsymmetrical ZnO rod having large surface area which or that can be seen in SEM micrograph and this was comparable

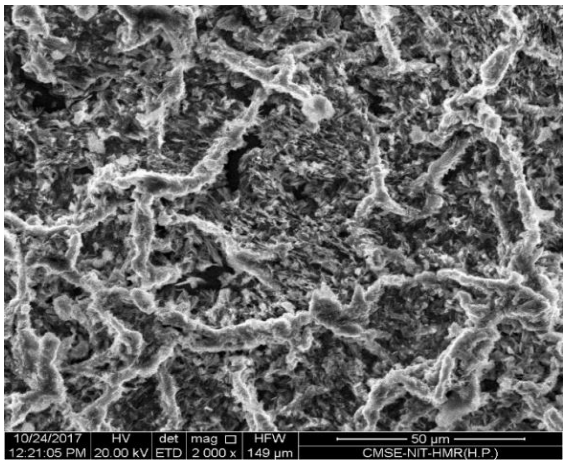

a

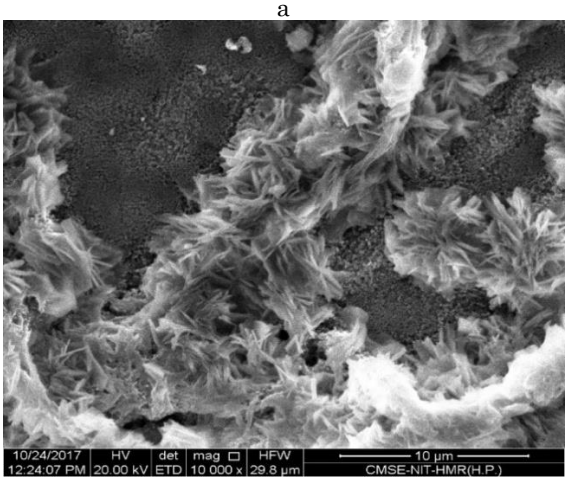

b

Fig. 2 – SEM image of ZnO thin film sample prepared at temperature 350 °C

with literature [21]. Figure 2 (b) show the image of sample prepared at 350 °C for 2 hr without any additional agent. The SEM images of the ZnO thin film prepared with different reaction times are presented below in Figure 3 (b). It can be seen that the morphology of the ZnO structures prepared by different temperatures showed similar spindle-shaped/flower structures having size 5.38 μm. That is, the reaction time had little effect on the morphology of the product. This image appears as a large area of spindle ZnO. The morphologies of ZnO nanostructure are diverse from each other. The density of ZnO nano crystal is relatively low, only little spindly crystal reunited into flower in the present concentration which we used in our experiment. When concentration is little higher, the density of ZnO nano crystals are appropriately, they are clearly visible as compared with the literature [22].

Surface morphology of ZnO thin film capped with polyvinyl alcohol is shown in Figure 3 (a and b). From the Figure 4 in the picture their morphology is not homogeneous. Even the appearance of the films does not look good, their surface is not uniform and there are many cracks and bubbles as compare with the literature [23]. The ZnO nanoparticles are clearly seen. The size of these spheres is

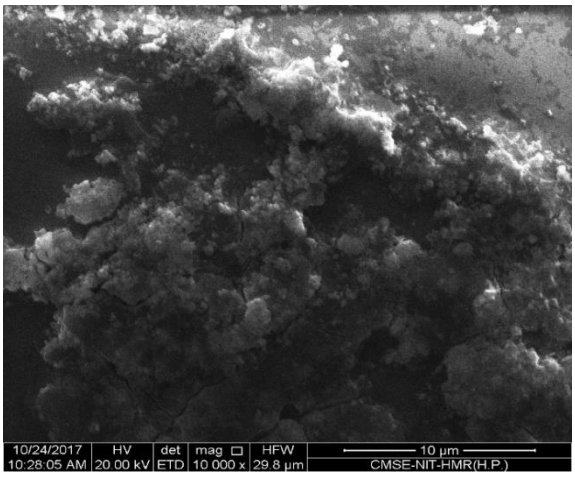

a

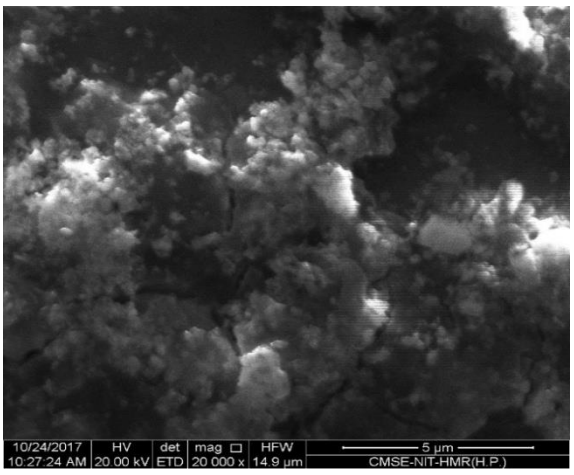

b

Fig. 3 – SEM image of ZnO thin film sample prepared at temperature 400 °C (With capping agent)

2.36 μm. Thus, capping agent affect the size of grains. Figures 3 (a) and (b) depict the SEM images of ZnO nanostructure with PVA as a capping agent annealed at temperatures 400 °C, respectively. With increasing annealing temperatures, the grain growth is observed in both samples as compared with the literature [24]. From micrograph, it is observed that growth of small square shape. Such type of square slabs in ZnO thin films are also observed by L. Znaidi et al. [25].

Table 1 show the grain size and shape of ZnO thin film which was deposited at different annealing temperatures.

3.2 UV-VIS Spectroscopy

Ultraviolet-Visible spectroscopy is used to analyze materials in the UV (200 to 400 nm) and visible (400 to 800 nm) region of the electromagnetic spectrum. UV-VIS transmittance characterization was used on ZnO thin film to investigate their optical properties. UV Spectrophotometer is employed in this work to characterize the optical properties of the fabricated samples. In this work we used to scan the samples in the wavelength range of 200-800 nm as shown in Figure 4.

Table 1 – Grain shape and size of ZnO thin films deposited at different annealing temperatures

№	Sample Condition	Shape	Size
1	Sample prepared at 300 °C	Nanoplates	1 μm
2	Sample prepared at 350 °C	Flower like shape	5.38 μm
3	Sample prepared at 400 °C (With capping agent)	Spherical shape	2.36 μm

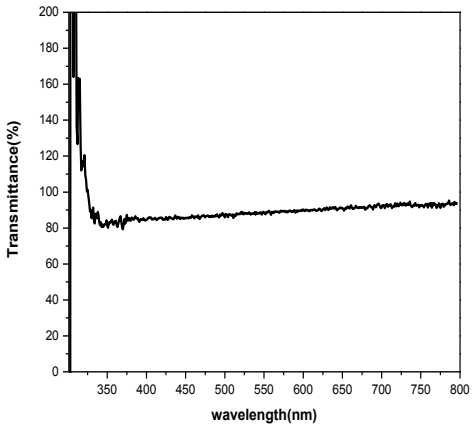

Fig. 4 – Optical transmittance spectrum of ZnO thin film sample annealed at temperature 400 °C (with capping agent)

As we noted that ZnO thin film shows not very good uniformity, but good surface passivation and chemical stability. Higher ZnO concentration in the solutions will promote aggregation to affect UV absorption and scatter visible light. This sample did not show intense absorption bands in this UV-Vis region, which indicates that the presence of ZnO in the thin film modified the optical properties.

The optical band gap energy E_g and absorption coefficient α is related by the equation (Tauc, 1970) [26].

$$(\alpha h\nu)^2 = A(h\nu - E_g)$$

Where α is the absorption coefficient, A is the constant, h is the Planck's constant, $h\nu$ is the photon energy, E_g is the optical band gap energy. The plot of square of the absorption coefficient vs. photon energy of the films prepared by different annealing temperatures is shown in the Figure 5, Figure 6 and Figure 7.

The energy gap E_g of the samples were evaluated from the intercept of the linear portion of the each curve for different annealing temperature with the $h\nu$ in X-axis.

Figure 5, 6, and 7 shows the relation between absorption edges $(\alpha h\nu)^2$ for PVA capped ZnO thin film as a function of photon energy $h\nu$. At extension of the curve to the value $(\alpha h\nu)^2 = 0$, we get the direct band gap of the zinc oxide thin film. The band gap energy E_g of PVA capped ZnO thin film is found to be 3.17 eV [27, 28]. The increase of transmission with increasing concentration can be due to a more enhanced crystallinity at higher precursor concentration and/or a decreasing optical scattering caused by densification of film crystallites. As the concentration increased, the grain size is also increased, and the grain boundary density of a film is decreased; therefore, the scattering of carriers at grain boundaries is decreased. The higher transmission

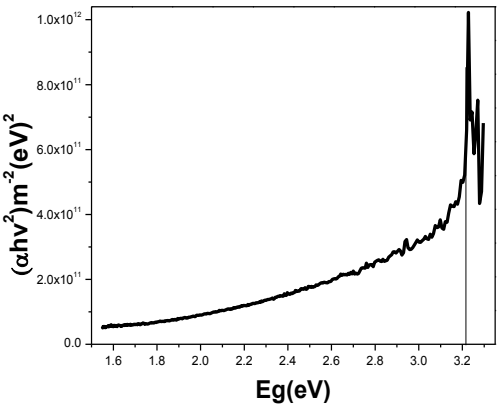

Fig. 5 – Typical $(\alpha h\nu)^2$ vs $(h\nu)$ shows optical band gap of sample annealed at 300 °C temperature

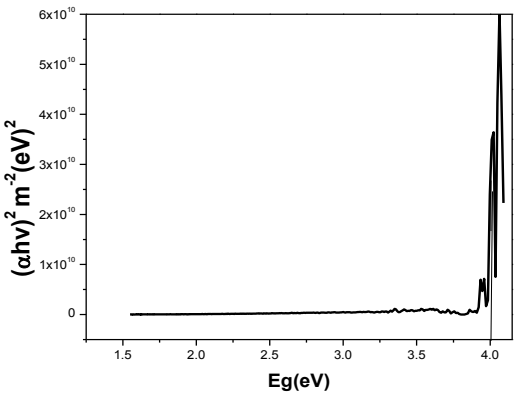

Fig. 6 – Typical $(\alpha h\nu)^2$ vs $(h\nu)$ shows optical band gap of sample annealed at 350 °C temperature

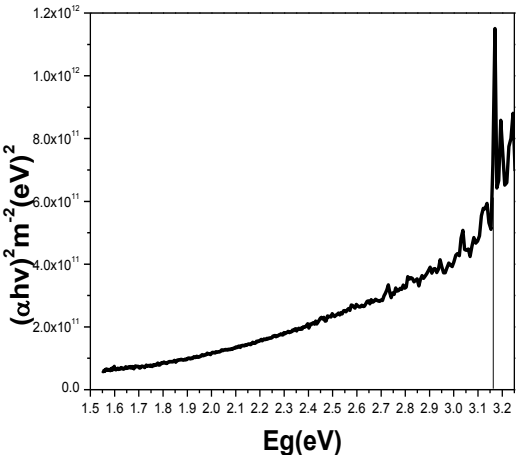

Fig. 7 – Typical $(\alpha h\nu)^2$ vs $(h\nu)$ shows optical band gap of sample annealed at 400 °C temperature

Table 2 – Grain shape and size of ZnO thin films deposited at different annealing temperatures

No	Annealing Temperature (°C)	Transmittance (%)	Band Gap (eV)
1	300 °C	< 60 %	3.23
2	350 °C	< 60 %	4.11
3	400 °C with capping agent PVA	< 80 %	3.17

reveals the impacts of precursor concentration on the optical property [29, 30].

It is observed that band gap is tuned in reasonable limit with capping agent and annealing temperatures 3.17-4.11 eV. Transparency as large as 80 % is achieved which is quite encouraging by this low cost method [28]. Table 2 gives values of E_g of the films deposited at different annealing temperatures.

Above studies suggest the suitability of ZnO transparent layers for optoelectronic applications. Dip coating looks a suitable low cost method for the deposition of such oxide layers, which has potential to scale up to industry level.

4. CONCLUSION

ZnO thin films have been grown on glass substrates by dip coating technique and film have been characterized for optical and structural measurements. All the films exhibit high transmittance in the range of 300 nm to 800 nm thus making the films suitable for optoelectronic devices, for instance as window layers in solar cells. It is clear from the SEM micrograph that the ultrathin flake-like nanostructures have grown on layer. ZnO nanoplatelets or nanoflakes like structure were formed on adding specific amount of zinc acetate dehydrated in the above precursors. In addition, network like porous structure was obtained because of low temperature growth. The film surface is not uniform and there are many cracks and bubbles. The sample which is prepared by zinc acetate dehydrated and potassium hydroxide 300 °C shows nanorods like structure and small grain. The other sample which is at 350 °C shows spindle like morphology of the sample, prepared by dip

coating method. The band gap of the sample is observed in the range 3.23 eV, 4.11 eV and 3.17 eV. The films showed transparency (< 80 %) in the visible region. Transmittance spectra show the transparency is not so much good. Above study suggest suitability of dip coating method for ZnO thin film for low cost optoelectronic devices.

REFERENCE

1. B. Ismail, M. Abaab, B. Rezig, *Thin Solid Films* **383**, 92 (2001).
2. Z.M. Jarzebzki, *Oxide Semiconductors* (Ed. by R.B. Pamplin) (Pergamon Press: Oxford: 1973).
3. R. Jayakrishnan, G. Hodes, *Thin Solid Films* **440**, 19 (2003).
4. D.J. Goyal, C. Agashe, M.G. Takwale, B.R. Marathe, V.G. Bhide, *J. Mater. Sci.* **4705**, 27 (1992).
5. A. Sanchez-Juarez, A. Tiburcio Silver, A. Ortiz, *Sol. Enegy Mater. Sol. C.* **52**, 301 (1998).
6. S. Ezhilvalavan, T.R.N. Kutty, *Mater. Chem. Phys.* **49**, 258 (1997).
7. M. de la L. Olvera, R. Asomoza, *Sensor. Actuat. B* **45**, 49 (1997).
8. R. Bhatt, H. Sankaranarayanan, C.S. Ferekides, D.H. Morel, *Proceedings of the 26th PVSC, 171, Anaheim, California*, p. 383 (1997).
9. J.A. Sans, A. Segura, M. Mollar, B. Mari, *Thin Solid Films* **453–454**, 251 (2004).
10. Y. Kashiwaba, F. Katahira, K. Haga, T. Sekiguchi, H. Watanabe, *J. Crystal Growth* **221**, 431 (2000).
11. D.F. Paraguay, L.W. Estrada, N.D.R. Acosta, E. Andrade, M. Miki-Yoshida, *Thin Solid Films* **350**, 192 (1999).
12. M.N. Kamalasanan, S. Chandra, *Thin Solid Films* **288**, 112 (1996).
13. J. Cembrero, A. Elmanouni, B. Hartiti, M. Mollar, B. Marí, *Thin Solid Films* **451–452**, 198 (2004).
14. V. Musat, B. Teixeira, E. Fortunato, R.C.C. Monteiro, *Thin Solid Films* **502**, 219 (2006).
15. S.Y. Kuo, W.C. Chen, F.-I. Lai, C.P. Cheng, H.C. Kuo, S.C. Wang, W.F. Hsieh, *J. Crystal Growth* **287**, 78 (2006).
16. Hongfong Ma, Fang Ma, Tao Zhao, Rongyan Jiyag, Hua Sun, *Sol. Energy Mater. Sol. C.* **137**, 73 (2015).
17. F. Shi, C.W. Cui, *Appl. Surf. Sci.* **256**, 2626 (2010).
18. C. Patarani, I.W. Lenggero, K. Okuyama, *J. Nanoparticle Res.* **5** No 1-2, 47 (2003).
19. Y. Wang, *Mater. Chem. Phys.* **153**, 266 (2015).
20. L. Znaidi, G.J.A.A.S. Illia, S. Benyahia, C. Sanchez, A.V. Kanaev, *Thin Solid Films* **428**, 257 (2003).
21. Zhenfei Zhang, Hairui Lui, Hua Zhang, *Superlattice. Microstructure.* **65**, 134 (2014).
22. Zohra Nazir Kayani, Maryam Iqbal, Saira Riaz, Rehana Zia, Shahzad Naseem, *Mater. Sci.-Pol.* **33** No 3, 515 (2015).
23. Nanda Shakti, P.S. Gupta, *Appl. Phys. Res.* **2** No 1, 19 (2010).
24. A.N. Mallika, A. Ramachandra Reddy, K. Venugopal Reddy, *J. Adv. Ceram.* **4** No 2, 123 (2015).
25. L. Znaidi, G.J.A.A.S. Illia, S. Benyahia, C. Sanchez, A.V. Kanaev, *Thin Solid Films*, **428**, 257 (2003).
26. J. Tauc, *The Optical Properties of Solids* (North-Holland: Amsterdam: 1970).
27. P.D. Cozzoli, L. Manna, M.I. Curri, *Chem. Mater.* **17**, 1296 (2005).
28. Sk. Muntaz Begum, K. Ravindranadh, R.V.S.S.N. Ravikumar, M.C. Rao, *Mater. Res. Inov.* **22** No 1, 37 (2016).
29. M. Smirnov, C. Baban, G.I. Rusu, *Appl. Surf. Sci.* **256**, 2405 (2010).
30. S.-Y. Kuo, W.-C. Chen, C.-P. Cheng, *Superlattice. Microstructure.* **39**, 162 (2006).